

Disorder-Induced Freezing of Dynamical Spin Fluctuations in Underdoped Cuprate Superconductors

Brian M. Andersen,¹ Siegfried Graser,^{2,3} and P.J. Hirschfeld³

¹*Niels Bohr Institute, University of Copenhagen, Universitetsparken 5, DK-2100 Copenhagen, Denmark*

²*Theoretical Physics III, Center for Electronic Correlations and Magnetism, Institute of Physics, University of Augsburg, D-86135 Augsburg, Germany*

³*Department of Physics, University of Florida, Gainesville, Florida 32611, USA*

(Received 4 May 2010; revised manuscript received 9 August 2010; published 28 September 2010)

We study the dynamical spin susceptibility of a correlated d -wave superconductor (dSC) in the presence of nonmagnetic disorder, using an unrestricted Hartree-Fock approach. This model provides a concrete realization of the notion that disorder slows down spin fluctuations, which eventually “freeze out.” The evolution of disorder-induced spectral weight transfer agrees qualitatively with experimental observations on underdoped cuprate superconductors. For sufficiently large disorder concentrations, static spin density wave (SDW) order is created when droplets of magnetism nucleated by impurities overlap. We also study the disordered stripe state coexisting with a dSC and compare its magnetic fluctuation spectrum to that of the disorder-generated SDW phase.

DOI: 10.1103/PhysRevLett.105.147002

PACS numbers: 74.25.Ha, 74.72.-h, 75.10.Jm, 75.40.Gb

Introduction.—Recent studies of layered high- T_c superconductors have provided evidence for nematic order of the underlying electronic state [1–5]. This development has reinvigorated studies of stripe phases in the cuprate materials and shown the important role of disorder. Here we focus on the magnetic excitations within a model that allows explicitly for disorder-induced pinning of incommensurate (IC) spin fluctuations [6]. Remarkable experimental progress in recent years has provided a converging picture of an hourglasslike dispersion of IC magnetic fluctuations which appear to be universal except for a low-energy branch which depends, e.g., on doping and material-specific parameters [7]. All materials appear to exhibit a spin-gap beyond some critical hole concentration x_c . By contrast, in the underdoped regime, the fluctuations soften and eventually freeze out to form a glassy spin state. This doping dependence seems to apply to both “clean” cuprates like $\text{YBa}_2\text{Cu}_3\text{O}_{6+x}$ (YBCO) where quasistatic spin density wave (SDW) order is found [3,8–11] and intrinsically disordered materials like $\text{La}_{2-x}\text{Sr}_x\text{CuO}_2$ (LSCO) where the static spin correlations are long range and persist for a large doping range well into the d -wave superconductor (dSC) dome [12]. The spin gap in the clean materials appears to persist to substantially lower doping, however.

Experimentally, it is known that an applied magnetic field or impurity substitution causes additional slowing down of spin fluctuations [13–19]. For example, in Ref. [17] it was shown how substitution of nonmagnetic Zn ions for Cu in 15% doped LSCO shifted spectral weight into the spin gap, and eventually, for enough Zn ($\sim 2\%$), generated elastic magnetic peaks in the neutron response. Upon increased temperature T the elastic signal decreases and eventually vanishes near T_c similar to an equivalent

disorder signal in Zn-free LSCO [15,20]. In $\text{YBa}_2(\text{Cu}_{1-y}\text{Zn}_y)_3\text{O}_{6.97}$ with $y = 2\%$, evidence for a similar in-gap Zn-induced mode was observed by Sidis *et al.* [21]. These results are consistent with slowing down and subsequent freezing seen by muon spin relaxation (μSR) in underdoped cuprates [22] and agrees with the overall picture from NMR studies that Zn ions not only suppress dSC but also strongly enhance SDW correlations [23]. Recent neutron scattering off detwinned $\text{YBa}_2\text{Cu}_3\text{O}_{6.6}$ with 2% Zn found induced short-range magnetic order and a redistribution of spectral weight from the resonance peak to uniaxial IC spin fluctuations at lower energies [24].

Theoretically, the hourglass spin dispersion has been studied within various stripe models [25,26], but a quantitative description including both spin and charge degrees of freedom, domain formation, glassiness, and/or slow fluctuations is still lacking. Some of these issues have been addressed recently [26–32], but modeling the dynamics of the neutron response in the presence of disorder remains limited at present [26,30,33].

Here, we focus on the disorder-induced magnetic phase known to exist in a correlated dSC [30] and calculate the dynamical spin susceptibility. For a homogeneous dSC our model reduces to a system of Bogoliubov quasiparticles whose magnetic response depends crucially on the presence of a dSC gap [34]. In the following, we investigate the role of spatially inhomogeneous local moments induced in this quasiparticle system; i.e., our formalism includes both the spin susceptibility from the dSC condensate and the local moments. Thus it goes beyond a spin-only approach by also including the charge carriers important for these metallic systems. A main goal of the calculation is to elucidate the spin fluctuation spectrum from a SDW droplet phase and compare it to the disordered stripe phase.

Model.—The Hamiltonian defined on an $L \times L$ lattice is

$$\hat{H} = - \sum_{ij\sigma} t_{ij} \hat{c}_{i\sigma}^\dagger \hat{c}_{j\sigma} + \sum_i (V_i - \mu) \hat{n}_i + U \sum_{i\sigma} \frac{n_i - \sigma m_i}{2} \hat{n}_{i\sigma} + \sum_{ij} (\Delta_{ij} c_{i\uparrow}^\dagger c_{j\downarrow}^\dagger + \Delta_{ij}^* c_{j\downarrow} c_{i\uparrow}), \quad (1)$$

where $\hat{c}_{i\sigma}^\dagger$ creates an electron on site i with spin σ , and $t_{ij} = \{t, t'\}$ denote the two nearest neighbor hopping integrals, μ is the chemical potential, and Δ_{ij} is the d -wave pairing potential between nearest neighbor sites i and j . The amplitude of Δ_{ij} is set by the dSC coupling constant g . The disorder potential V_i is generated from N randomly positioned pointlike scatterers of strength $V = 100t$, yielding the disorder concentration $n_{\text{imp}} = N/L^2$. This particular choice of potential is meant to mimic strong nonmagnetic substitutional impurities [24], but we expect that results qualitatively similar to those presented below may also be obtained for weaker scatterers relevant for modeling, e.g., dopant impurities [30]. We fix the parameters $t' = -0.35t$, $g = 0.3t$ leading to pairing amplitudes $\Delta \sim 0.1t$ and adjust μ to give a hole doping $x = 1 - n \simeq 0.13$. We solve Eq. (1) self-consistently on unrestricted lattices ($L = 24$) by diagonalizing the associated Bogoliubov–de Gennes (BdG) equations at $T = 0$ [35].

Equation (1) has been used previously to study, e.g., moment formation around nonmagnetic impurities [36]. In the case of many impurities, it was used to model static disorder-induced magnetic droplets [27,31,32] and to explain how these may increase in volume fraction when moving to lower doping and eventually form a SDW long-range ordered phase [30,33].

The transverse bare spin susceptibility $\chi_0^{xx}(\vec{r}_i, \vec{r}_j, \omega) = -i \int_0^\infty dt e^{i\omega t} \langle [\sigma_i^x(t), \sigma_j^x(0)] \rangle$ can be expressed in terms of the BdG eigenvalues E_n and eigenvectors u_n, v_n as

$$\chi_0^{xx}(\vec{r}_i, \vec{r}_j, \omega) = \sum_{m,n} f(u, v) \frac{f(E_m) + f(E_n) - 1}{\omega + E_m + E_n + i\Gamma} + \sum_{m,n} g(u, v) \frac{f(E_m) + f(E_n) - 1}{\omega - E_m - E_n + i\Gamma}, \quad (2)$$

where $f(u, v) = u_{m,i}^* v_{n,i}^* (u_{m,j} v_{n,j} - u_{n,j} v_{m,j})$ and $g(u, v) = v_{m,i} u_{n,i} (u_{m,j}^* v_{n,j}^* - u_{n,j}^* v_{m,j}^*)$. Including interactions within RPA the full susceptibility then reads

$$\chi^{xx}(\vec{r}_i, \vec{r}_j, \omega) = \sum_{\vec{r}_l} [1 - U \chi_0^{xx}(\omega)]_{\vec{r}_i, \vec{r}_l}^{-1} \chi_0^{xx}(\vec{r}_l, \vec{r}_j, \omega). \quad (3)$$

Fourier transforming with respect to the relative coordinate $\vec{r} = \vec{r}_i - \vec{r}_j$ defines the spatially resolved momentum-dependent susceptibility $\chi(\vec{R}, \vec{q}, \omega) = \sum_{\vec{r}} e^{i\vec{q} \cdot \vec{r}} \chi(\vec{R}, \vec{r}, \omega)$. Averaging over the center of mass coordinate $\vec{R} = (\vec{r}_i + \vec{r}_j)/2$ gives the susceptibility $\chi(q, \omega)$ relevant for comparison with neutron measurements.

Results.—The Hamiltonian (1) supports both a correlation- and disorder-induced SDW phase. Specifically, in the clean case above a critical repulsion $U_{c2} \simeq 2.75t$ a global stripe phase is the favorable state. Below U_{c2} the ground state is a homogeneous dSC, but nonmagnetic disorder may locally induce moments if $U > U_{c1}$, where U_{c1} is another critical interaction strength [30,35]. In Fig. 1 we show the magnetization and spin susceptibility in the clean system for $U < U_{c2}$ [Figs. 1(a) and 1(b)] and $U > U_{c2}$ [Figs. 1(c) and 1(d)]. Figures 1(a) and 1(b) are homogeneous dSCs, whereas the stripe phase in Figs. 1(c) and 1(d) coexists with a stripe-modulated dSC order parameter. The spin susceptibility in Fig. 1(a) is dominated by a spin-1 in-gap resonance mode whose very existence depends crucially on the presence of a dSC gap [34]. By contrast, the spin-wave branches in the ordered case in Fig. 1(c) are independent of the presence of a coexisting dSC condensate.

We now demonstrate how disorder masks the clear distinction between the susceptibilities in Figs. 1(a) and 1(c). This is evident from Fig. 2 showing the evolution of the spectrum in Fig. 1(a) as a function of increased disorder concentrations n_{imp} . One clearly sees the impurity-induced low-energy spectral weight entering the legs of the lower part of the hourglass, as well as an overall shifting down and broadening of the dispersion branch. The shift is seen more clearly in Figs. 3(a)–3(c), which show ω cuts at $q_{1C} = (\frac{3}{4}, 1)\pi$ for various values of U and n_{imp} . At lower U , impurity concentrations of just a few percent may strongly enhance the low-energy weight and generate an in-gap mode [Figs. 3(a) and 3(b)], in agreement with neutron scattering on Zn-substituted samples and in applied fields [17,19,21,24,37]. For sufficiently large disorder concentrations n_{imp} and repulsion U , the static component dominates $\chi(q_{1C}, \omega)$, as shown in Fig. 3(c).

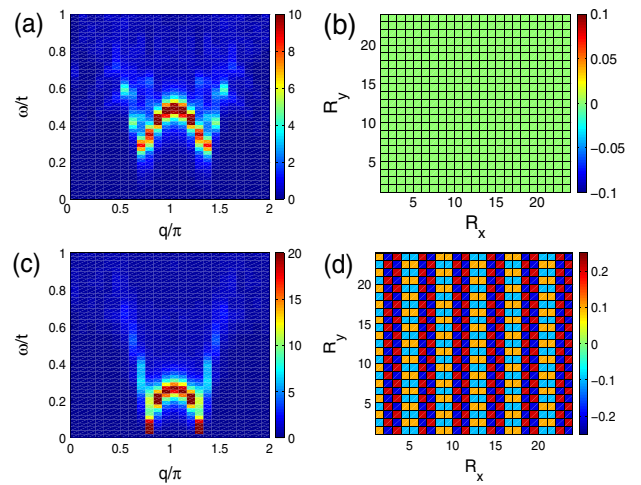


FIG. 1 (color online). Intensity plot of $\chi(q, \omega)$ along a cut $\vec{q} = (q, \pi)$ (a),(c) and magnetization (b),(d) in the clean system with (without) stripes shown in (a),(b) [$U = 2.6t$] [(c), (d) [$U = 2.9t$]]. The susceptibility in (c) is the sum of $\chi(q, \pi, \omega)$ and $\chi(\pi, q, \omega)$ representing domain averaging.

The low-energy weight shown in Figs. 2 and 3 arises from the disorder-induced magnetism as can be directly verified by the spatial information contained in $\chi(q, R, \omega)$. Figures 3(e) and 3(f) display both $\chi(q_{1C}, R, \omega)$, with R being a nearest neighbor site of a single nonmagnetic impurity, and the R -averaged dynamical susceptibility $\chi(q_{1C}, \omega)$ for $U < U_{c1}$ [Fig. 3(e)] and $U > U_{c1}$ [Fig. 3(f)]. The local SDW droplet induced by the impurity is shown in Fig. 3(d). From Fig. 3(f) it is evident that the neighboring sites to the impurity exhibit a low-energy peak which is directly responsible for the low-energy weight in the spatially averaged $\chi(q_{1C}, \omega)$.

Figures 2 and 3 apply to the so-called droplet phase where the system spontaneously generates impurity-induced local SDW puddles as shown in the right-hand panels of Fig. 2. Note that the susceptibility presented here is for a few percent strong scatterers representing, e.g., Zn, but that the overall phenomenology may also apply to intrinsically disordered cuprates like LSCO and BSCCO [30,33].

In the remainder we turn to the limit where $U > U_{c2}$ and compare the results obtained above to a disordered stripe phase [26–33]. Figures 4(a) and 4(b) show how the magnetization from Fig. 1(d) evolves into a nematic phase when disorder destroys the translational invariance. For a discussion of the disorder effects on the spin spectrum it is

convenient to look separately at the dispersion perpendicular [Figs. 4(c) and 4(d)] and parallel [Figs. 4(e) and 4(f)] to the stripe direction. In the limit of low disorder [Figs. 4(a), 4(c), and 4(e)] the spin fluctuations are qualitatively similar to the clean stripe case from Fig. 1(c) (which shows the directional-averaged susceptibility). When sufficient disorder is added, the stripes break up and meander strongly, which is revealed in the spin response as a significant broadening of the high-energy part of the hourglass including the spin resonance at (π, π) and a shifting down of spectral weight in the response parallel to the stripe direction as seen from Fig. 4(f). A natural question arising from the similarity between the spin spectrum in the droplet phase [see, e.g., Fig. 2(e)] and the disordered stripe phase in Fig. 4 is how to experimentally distinguish between them. Since the droplet phase preserves the C_4 symmetry of the underlying lattice, whereas the stripe phase breaks C_4 to C_2 , which remains robust even with significant disorder, we find that $q_x - q_y$ anisotropy in the neutron response is the best way to answer this question. Experiments on detwinned underdoped YBCO samples

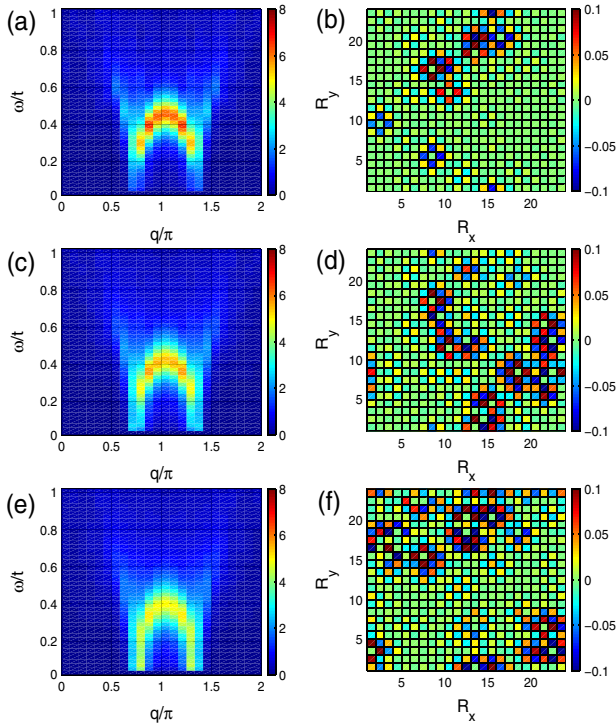


FIG. 2 (color online). (a),(c),(e) Same as in Fig. 1(a) with the addition of disorder. Panels (b),(d),(f) show the associated real-space static magnetization. Parameters are $U = 2.6t$ and $n_{\text{imp}} \approx 1\%$ (a),(b), $n_{\text{imp}} \approx 2\%$ (c),(d), and $n_{\text{imp}} \approx 3\%$ (e),(f). The results in the left-hand panels are averaged over ten random disorder configurations.

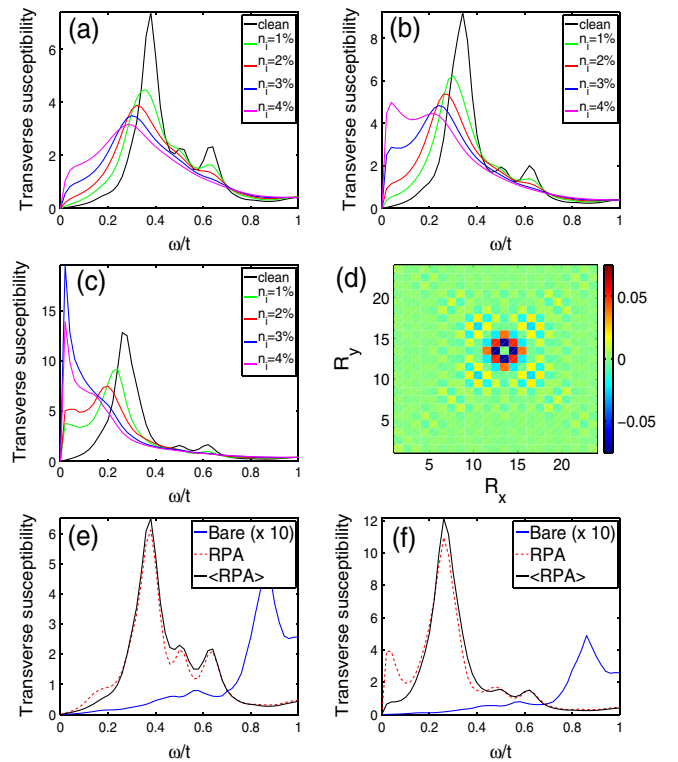


FIG. 3 (color online). (a)–(c) $\chi(q_{1C}, \omega)$ as a function of ω for different n_{imp} and $U = 2.5t$ (a), $U = 2.6t$ (b), and $U = 2.7t$ (c). Panel (d) shows the real-space magnetization induced by a single nonmagnetic impurity at $R = (12, 12)$ for $U = 2.7t$. Panels (e), (f) display the susceptibility at the IC wave vector $q_{1C} = (\frac{3}{4}, 1)\pi$ in the bare ($U = 0$) case (blue solid curve) and the full local susceptibility at $R = (11, 12)$ (red dashed line) with $U = 2.5t < U_{c1}$ (e) and $U = 2.7t > U_{c1}$ (f). The black solid lines in (e),(f) show the spatially averaged full RPA susceptibility $\chi(q_{1C}, \omega)$.

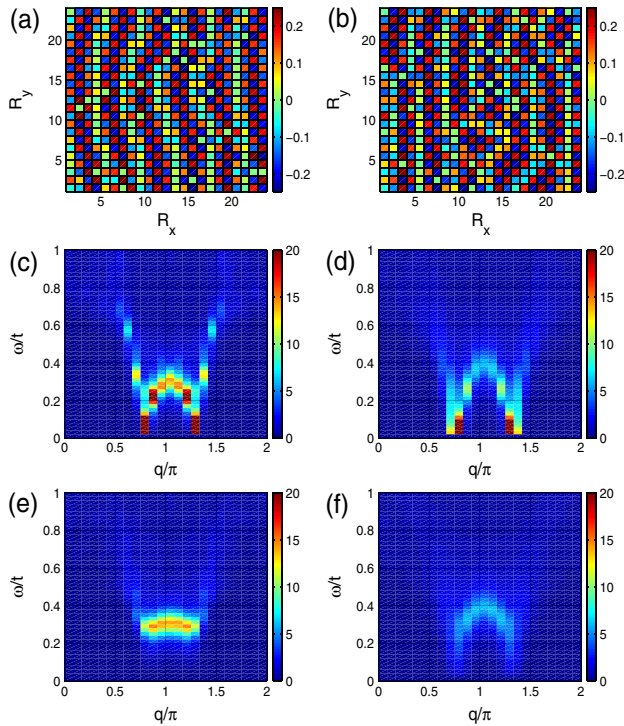


FIG. 4 (color online). (a),(b) Real-space magnetization with 2% (a) and 4% (b) disorder added to a stripe ordered system similar to Fig. 1(d). Panels (c)–(f) show the associated susceptibility transverse (c),(d) and along (e),(f) the stripe direction for the same impurity concentrations, i.e., 2% disorder in (c),(e) and 4% in (d),(f).

have recently reported such anisotropy in the low-energy intrinsic [3] and Zn-induced spectral weight [24]. We suggest that future experiments on samples with tetragonal crystal symmetry should be performed to test for similar anisotropy. Careful studies of any potential anisotropy in the inelastic signal may also reveal to what extent the droplet phase can be viewed as a precursor of the stripe phase [33].

Conclusions.—We have studied disorder effects on the hourglass spin fluctuation spectrum relevant for the cuprates. We have focused on two regimes of electronic repulsion U leading to a magnetic droplet phase for low U and a disordered stripe phase at larger U . Within this scenario, it is likely that the underdoped state is well described by our results for larger U , since we expect that the effective interaction scale U/t increases as one approaches the Mott limit. We have also shown how neutron studies of detwinned samples may be used to distinguish between them despite their surprisingly similar fluctuation spectrum in as-grown samples.

B.M.A. acknowledges support from The Danish Council for Independent Research–Natural Sciences. S.G. acknowledges support from the DFG through TRR 80. P.J.H. received partial support from the U.S. Department of Energy under Grant No. DE-FG02-05ER46236.

- [1] Y. Ando *et al.*, *Phys. Rev. Lett.* **88**, 137005 (2002).
- [2] R. Daou *et al.*, *Nature (London)* **463**, 519 (2010).
- [3] V. Hinkov *et al.*, *Science* **319**, 597 (2008).
- [4] M. Matsuda *et al.*, *Phys. Rev. Lett.* **101**, 197001 (2008).
- [5] M. J. Lawler *et al.*, *Nature (London)* **466**, 347 (2010).
- [6] S. A. Kivelson *et al.*, *Rev. Mod. Phys.* **75**, 1201 (2003).
- [7] J. M. Tranquada, in *Handbook of High-Temperature Superconductivity Theory and Experiment*, edited by J. R. Schrieffer (Springer, New York, 2007).
- [8] C. Stock *et al.*, *Phys. Rev. B* **73**, 100504(R) (2006).
- [9] J. Sonier *et al.*, *Phys. Rev. B* **76**, 064522 (2007).
- [10] S. Li *et al.*, *Phys. Rev. B* **77**, 014523 (2008).
- [11] D. Haug *et al.*, *Phys. Rev. Lett.* **103**, 017001 (2009).
- [12] M.-H. Julien, *Physica (Amsterdam)* **329–333B**, 693 (2003).
- [13] K. Hirota *et al.*, *Physica (Amsterdam)* **241–243B**, 817 (1997).
- [14] S. Katano *et al.*, *Phys. Rev. B* **62**, R14677 (2000).
- [15] B. Lake *et al.*, *Nature (London)* **415**, 299 (2002).
- [16] B. Khaykovich *et al.*, *Phys. Rev. B* **66**, 014528 (2002).
- [17] H. Kimura *et al.*, *Phys. Rev. Lett.* **91**, 067002 (2003).
- [18] A. T. Savici *et al.*, *Phys. Rev. Lett.* **95**, 157001 (2005).
- [19] J. Chang *et al.*, *Phys. Rev. Lett.* **102**, 177006 (2009).
- [20] H. Kimura *et al.*, *Phys. Rev. B* **59**, 6517 (1999).
- [21] Y. Sidis *et al.*, *Phys. Rev. B* **53**, 6811 (1996).
- [22] P. Mendels *et al.*, *Phys. Rev. B* **49**, 10035 (1994); C. Bernhard *et al.*, *ibid.* **58**, R8937 (1998); Ch. Niedermayer *et al.*, *Phys. Rev. Lett.* **80**, 3843 (1998); I. Watanabe *et al.*, *Phys. Rev. B* **65**, 180516(R) (2002); C. Panagopoulos *et al.*, *ibid.* **66**, 064501 (2002).
- [23] A. V. Mahajan *et al.*, *Phys. Rev. Lett.* **72**, 3100 (1994).
- [24] A. Suchaneck *et al.*, *Phys. Rev. Lett.* **105**, 037207 (2010).
- [25] F. Krüger and S. Scheidl, *Phys. Rev. B* **67**, 134512 (2003); M. Vojta and T. Ulbricht, *Phys. Rev. Lett.* **93**, 127002 (2004); G. S. Uhrig, K. P. Schmidt, and M. Grüninger, *ibid.* **93**, 267003 (2004); E. W. Carlson, D. X. Yao, and D. K. Campbell, *Phys. Rev. B* **70**, 064505 (2004); G. Seibold and J. Lorenzana, *Phys. Rev. Lett.* **94**, 107006 (2005); B. M. Andersen and P. Hedegård, *ibid.* **95**, 037002 (2005); B. M. Andersen and O. F. Syljuåsen, *Phys. Rev. B* **75**, 012506 (2007); R. M. Konik, F. H. L. Essler, and A. M. Tsvelik, *ibid.* **78**, 214509 (2008).
- [26] M. Vojta, T. Vojta, and R. K. Kaul, *Phys. Rev. Lett.* **97**, 097001 (2006).
- [27] G. Alvarez *et al.*, *Phys. Rev. B* **71**, 014514 (2005).
- [28] J. A. Robertson *et al.*, *Phys. Rev. B* **74**, 134507 (2006).
- [29] A. Del Maestro, B. Rosenow, and S. Sachdev, *Phys. Rev. B* **74**, 024520 (2006).
- [30] B. M. Andersen *et al.*, *Phys. Rev. Lett.* **99**, 147002 (2007).
- [31] W. A. Atkinson, *Phys. Rev. B* **75**, 024510 (2007).
- [32] B. M. Andersen and P. J. Hirschfeld, *Phys. Rev. Lett.* **100**, 257003 (2008).
- [33] M. Schmid *et al.*, *New J. Phys.* **12**, 053043 (2010).
- [34] I. Eremin *et al.*, *Phys. Rev. Lett.* **94**, 147001 (2005); M. R. Norman, *Phys. Rev. B* **75**, 184514 (2007); I. Eremin *et al.*, *Phys. Rev. B* **75**, 184534 (2007).
- [35] J. W. Harter *et al.*, *Phys. Rev. B* **75**, 054520 (2007).
- [36] H. Alloul *et al.*, *Rev. Mod. Phys.* **81**, 45 (2009).
- [37] B. M. Andersen, O. F. Syljuåsen, and P. Hedegård, *Phys. Rev. B* **80**, 052509 (2009).